

# Ho substitution suppresses collinear Dy spin order and enhances polarization in DyMnO<sub>3</sub>

N. Zhang,<sup>1,2</sup> Y. Y. Guo,<sup>1</sup> L. Lin,<sup>1</sup> S. Dong,<sup>3</sup> Z. B. Yan,<sup>1</sup> X. G. Li,<sup>4</sup> and J.-M. Liu<sup>1,5,a)</sup>

<sup>1</sup>Laboratory of Solid State Microstructures, Nanjing University, Nanjing 210093, China

<sup>2</sup>College of Physics and Information Engineering, Henan Normal University, Xinxiang, China

<sup>3</sup>Department of Physics, Southeast University, Nanjing 211189, China

<sup>4</sup>Department of Physics, University of Science and Technology of China, Hefei, Anhui 230026, China

<sup>5</sup>International Center for Materials Physics, Chinese Academy of Sciences, Shenyang, China

(Received 28 July 2011; accepted 20 August 2011; published online 9 September 2011)

The multiferroic behaviors of Dy<sub>1-x</sub>Ho<sub>x</sub>MnO<sub>3</sub> are investigated in order to reveal the effects of Ho-substitution on the independent collinear Dy spin order and ferroelectric polarization at low temperature. It is demonstrated that a partial Ho-substitution of Dy ions significantly suppresses the independent Dy spin order at low temperature on one hand, and maintains the R-Mn spin coupling on the other hand, thus leading to a remarkable enhancement of the polarization at low temperature.

© 2011 American Institute of Physics. [doi:10.1063/1.3636399]

The second class of multiferroics, in which the ferroelectricity is induced by particular magnetic orders, have been receiving special attentions since the discovery of gigantic magnetoelectric effect in TbMnO<sub>3</sub> and others.<sup>1-3</sup> For RMnO<sub>3</sub> (R = Tb, Dy, or Eu<sub>1-x</sub>Y<sub>x</sub>) and other similar materials, the Mn spiral spin order is essential for the onset of ferroelectric polarization  $P$ ,<sup>3-13</sup> which was understood in the framework of spin current scenario or inverse Dzyaloshinskii-Moriya interaction. The as-generated polarization can be expressed as  $P_{so} \sim \sum A e_{ij} \times (S_i \times S_j) \sim \langle S_i \times S_j \rangle$ , where  $e_{ij}$  denotes the unit vector connecting the two neighbor spins ( $S_i$  and  $S_j$ ), coefficient  $A$  is mainly relevant to the spin-orbit coupling, and  $\langle \dots \rangle$  denotes the configuration averaging.<sup>14-16</sup> This spin-orbit coupling mechanism offers us an alternative way to understand the ferroelectricity and its applications.

However, recent works revealed that the rare-earth (R) spin, which had been usually ignored in the above mentioned models,<sup>16,17</sup> might play substantial roles in modulating  $P$ . For example, for nonmagnetic (Eu,Y)MnO<sub>3</sub> series or less magnetoanisotropic GdMnO<sub>3</sub> where Gd has relatively small spin moment,<sup>3,10</sup> the measured  $P$  prefers to align along the  $a$ -axis, where it orients along the  $c$ -axis for strongly anisotropic (Tb,Dy)MnO<sub>3</sub>.<sup>3-9</sup> On the other hand, it was suggested that the strong coupling between the R spin and Mn spin (*hereafter* abbreviated as the R-Mn spin coupling) may also make substantial contribution to polarization  $P$ , particularly for DyMnO<sub>3</sub> (DMO).<sup>3-9</sup> Experimentally, the Dy spins begin to be polarized at temperature  $T$  below  $T_N \sim 39$  K, probably due to this strong coupling.<sup>7</sup> At  $T < T_{FE} \sim 18$  K, the Mn spins develop the spiral spin order and consequently the Dy spins arrange noncollinearly, coinciding with the onset of  $P$ .<sup>8</sup> In particular, the Dy spiral spin order has the same propagation vector ( $\tau$ ) as the Mn spiral spin order (i.e.,  $\tau^{Dy} = \tau^{Mn} = 0.385\mathbf{b}$  where  $\mathbf{b}$  is the lattice vector along the  $b$ -axis). This R-Mn spin coupling allows the symmetric exchange striction between the Dy sublattice and Mn sublattice, and thus represents the spin-lattice coupling. The as-generated polarization  $P_{sp}$  is propor-

tional to  $[S_R \cdot S_{Mn}]$ , where  $[\dots]$  denotes a specific site-dependent configuration averaging.<sup>3,8,9</sup> Therefore, the total polarization can be simply viewed as a sum of the two components, i.e.,  $P = P_{so} + P_{sp}$ . This picture is schematically illustrated in Fig. 1(a) with the Dy and Mn spins projected on the  $bc$ -plane for a guide of eyes.

Unfortunately, the Dy spiral spin order only exists in a finite  $T$ -range:  $T_{Dy} < T < T_{FE}$ . Below  $T_{Dy} \sim 7$  K, the Dy spin alignment is no longer subjected to the R-Mn spin coupling but develops its independent collinear antiferromagnetic (AFM) order, which has no contribution to  $P$ . The vanish of the induced Dy spiral spin order below  $T_{Dy}$  weakens  $P$  remarkably at low  $T$  by removing component  $P_{sp}$ ,<sup>4,5,7</sup> as shown in Fig. 1(b). Interestingly, it was reported that an external magnetic field ( $H$ ) can transform this independent collinear order into the spiral spin order with  $\tau^{Dy} = 0.385\mathbf{b}$ , leading to the field-induced enhancement of  $P$  below  $T_{Dy}$ .<sup>7</sup> This is also a clear evidence that the R-Mn spin coupling is never a negligible ingredient of the multiferroicity in RMnO<sub>3</sub>.

To avoid the  $P$  suppression of DMO at low  $T$ , an immediate approach is to partially substitute Dy with other R element so that the independent Dy spin order at low  $T$  can be melted away while the R-Mn spin coupling can be maintained. In fact, our earlier study<sup>18</sup> did suggest the collapse of the independent Dy spin order at low  $T$  upon the Y substitution. However, since Y ion is nonmagnetic, such a substitution weakens the R-Mn spin coupling either, thus suppressing the as-generated  $P_{sp}$ . Along this line, a magnetic R substitution of Dy seems more favorable, so long as this substituting element does not favor the independent spin order at low  $T$ . Furthermore, this magnetic substitution also allows a platform on which the R-Mn spin coupling as a general ingredient of the physics for polarization generation in multiferroic RMnO<sub>3</sub> beyond DMO can be checked. This motivation can be schematically shown in Figs. 1(c) and 1(d), where the R spins can align in a spiral spin order roughly synchronous to the Mn spiral spin order both at  $T_{Dy} < T < T_{FE}$  and below  $T_{Dy}$ , so that the exchange striction mechanism associated with  $[S_R \cdot S_{Mn}]$  works.

<sup>a)</sup> Author to whom correspondence should be addressed. Electronic mail: liujm@nju.edu.cn.

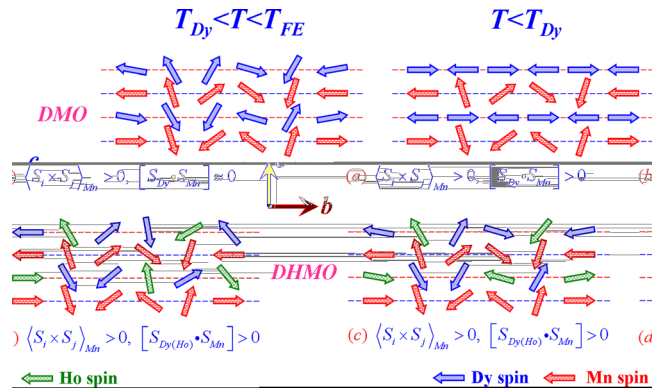


FIG. 1. (Color online) Schematic drawing of the Dy(Ho) and Mn spin configurations at  $T < T_{Dy}$  (right column) and  $T_{Dy} < T < T_{FE}$  (left column) for pure DMO (up row) and DHMO (bottom row). The magnitude and orientation of these spin arrows are drawn only for guide of eyes.

In this work, we address the above motivation, and choose partial substitution of Dy by Ho, i.e.,  $Dy_{1-x}Ho_xMnO_3$  (DHMO), based on the following reasons. First,  $Ho^{3+}$  ion has similar size as  $Dy^{3+}$  ion and their spin moments are similar in magnitude. Second, no independent Ho spin ordering in orthorhombic  $HoMnO_3$  was observed at low  $T$ ,<sup>3</sup> avoiding the independent Ho spin ordering at low  $T$  in DHMO. Third, the substitution level  $x$  is restricted within a low level ( $x \leq 0.3$ ) in order to exclude potential effects associated with the  $E$ -type AFM order favored in metastable orthorhombic  $HoMnO_3$ .

The polycrystalline DHMO samples were prepared from the mixture of  $Dy_2O_3(4N)$ ,  $Mn_2O_3(3N)$ , and  $Ho_2O_3(4N)$  using the standard solid-state reaction. The crystal structure was investigated at room temperature by  $x$ -ray diffraction (XRD) using  $Cu K_\alpha$  radiation. The magnetization ( $M$ ) and specific heat ( $C/T$ ) were measured using the Quantum Design superconducting quantum interference device magnetometer and physical properties measurements system (PPMS), respectively. Polarization  $P$  was measured using the pyroelectric current method (using Keithley 6514 electrometer) integrated with the PPMS. The opposite faces of platelet samples were sputtered with gold electrodes. As a poling procedure, each sample was first cooled down to 2 K under an electric field of 10 kV/cm, and then the pyroelectric current was detected at a  $T$ -sweeping rate of 2 K/min–6 K/min ( $H$ -sweeping rate of 100 Oe/s).

Figure 2 shows the measured XRD patterns of a series of as-prepared samples. All the reflections indicate that our samples do have a single orthorhombic structure with space group  $Pbnm$  and excellent crystallinity without second phase

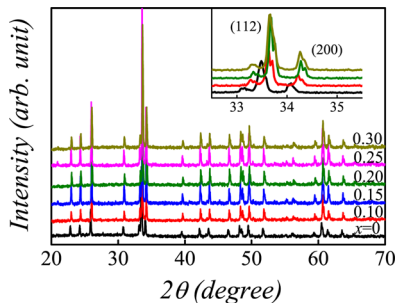


FIG. 2. (Color online) Room temperature XRD  $\theta$ - $2\theta$  patterns for a series of samples. The inset shows the (112) and (200) peaks for  $x=0, 0.1, 0.2,$  and  $0.3$  from bottom to up.

within the apparatus resolution. In comparison with DMO, the slight higher  $2\theta$ -side shift of the reflections with increasing  $x$  is observed, as identified in the inset of Fig. 2, indicating a slight lattice shrinking. This effect is reasonable considering the Ho ionic radius  $r_{Ho} \sim 0.901 \text{ \AA}$  smaller than Dy ion  $r_{Dy} \sim 0.912 \text{ \AA}$ .

We then perform the multiferroic characterization of the DHMO samples. The measured  $M$  and  $C/T$  as a function of  $T$  for several samples are plotted in Fig. 3, noting that  $M$  was measured under the zero-field-cooled (ZFC) and field-cooled (FC) conditions with  $H \sim 100$  Oe. For sample  $x=0$ , i.e., DMO, the magnetization is mainly contributed from the independent  $Dy^{3+}$  spin moment.<sup>4,5</sup> No anomaly in connection with the AFM transitions of  $Mn^{3+}$  spins can be detected. The only left anomaly in the ZFC  $M$ - $T$  curve is the peak at  $T_{Dy} \sim 6.5$  K, due to the independent  $Dy^{3+}$  spin ordering. Upon the substitution, the measured  $M$ - $T$  curves show that the anomaly occurring at  $T_{Dy}$  downshifts to low- $T$  side, as further displayed in the inset of Fig. 3(a), indicating the suppression of the independent Dy spin ordering.

Furthermore, the measured  $C/T$  data under zero-field condition are plotted in Fig. 3(b). As a reference, the  $C/T \sim T$  curve for sample  $x=0$  presents three sharp anomalies at  $T_N \sim 39$  K,  $T_{FE} \sim 18$  K, and  $T_{Dy} \sim 6.5$  K, attributed to the Mn collinear sinusoidal transition, the Mn spiral spin ordering plus the induced Dy spiral spin ordering associated with onset of ferroelectricity, and the Dy independent spin ordering, respectively.<sup>3-9</sup> Consistent with the  $M$ - $T$  data, the  $C/T$ - $T$  data show that the Ho-substitution results in the downshift of  $T_{Dy}$  with increasing  $x$ . This anomaly disappears at  $x > 0.2$ , revealing that the Dy independent spin order completely melts away as  $x > 0.2$ . Additionally, the Ho-substitution also modulates slightly the characteristic points,  $T_N$  and  $T_{FE}$ .

Subsequently, we look at  $P$  as a function of  $T$  for several samples, as shown in Fig. 4(a). First of all, for  $x=0$ , it is shown that the measured  $P$  does become seriously suppressed at  $T < T_{Dy}$ , due to the independent Dy spin ordering, while at  $T_{Dy} < T < T_{FE}$  the measured  $P$  sums the contributions from the Mn spiral spin order ( $P_{so}$ ) and the  $R$ -Mn spin coupling ( $P_{sp}$ ). Upon the substitution, on one hand, the measured  $P$  at low  $T$  ( $T < T_{Dy}$ ) obtains remarkable enhancement. The value of  $P$  at  $T=2$  K as a function of  $x$ , shown in the inset of Fig. 4(a), clearly evidences this effect. On the other hand, it is also identified that at  $T_{Dy} < T < T_{FE}$ , the Ho-substitution does not damage the measured  $P$  although a slight downward shift of the  $P$ - $T$  curve is observed. Furthermore, the responses of  $P$  against  $H$  at  $T=2$  K for samples  $x=0$  and  $0.1$  are shown in

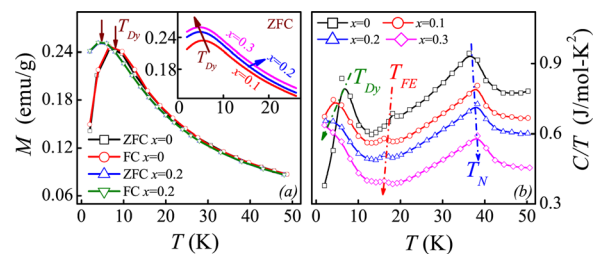


FIG. 3. (Color online) (a) Measured  $M$ - $T$  curves under ZFC and FC conditions for samples  $x=0$  and  $0.2$  (b) measured  $C/T$  as a function of  $T$  for samples  $x=0, 0.1, 0.2,$  and  $0.3$ .

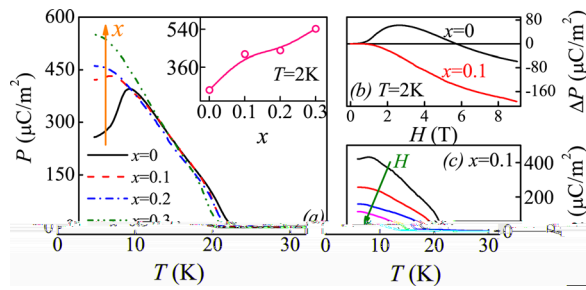


FIG. 4. (Color online) (a) Measured  $P$ - $T$  curves for samples  $x=0, 0.1, 0.2$ , and  $0.3$ , and the inset shows the measured  $P$  at  $T=2$  K as a function of  $x$ , (b) measured  $\Delta P$ - $H$  relations at  $T=2$  K for samples  $x=0$  and  $0.1$ , and (c) measured  $P$ - $T$  curves for various  $H$  (from top to bottom,  $H=0, 3T, 6T$ , and  $9T$ ) for sample  $x=0.1$ .

Fig. 4(b), where  $\Delta P = P(H) - P(0)$ . For  $x=0$ , the measured  $P$  is enhanced in the intermediate  $H$ -range and then suppressed when  $H$  is high enough, which is consistent with earlier reports.<sup>3,7,18</sup> However, for  $x=0.1$ , the measured  $P$  is monotonously suppressed with increasing  $H$ . This result is further confirmed by the  $T$ -dependence of  $P$  measured under various  $H$  for sample  $x=0.1$ , as presented in Fig. 4(c).

The above presented data confirm our motivation with respect to several aspects. First, the Ho-substitution does not damage the strong  $R$ -Mn spin coupling which contributes to polarization  $P$  via term  $[S_R \cdot S_{Mn}]$ , i.e., the exchange striction mechanism. Therefore, no damage of  $P$  at  $T_{Dy} < T < T_{FE}$  is detected. Second, the Ho-substitution does melt away the independent Dy spin order at low  $T$ , replaced with the Dy/Ho spiral spin order so as to the exchange striction mechanism works further down to  $T < T_{Dy}$ . Therefore, polarization  $P$  at low  $T < T_{Dy}$  is enhanced remarkably. Third, it is suggested that the  $R$ -Mn spin coupling, as a general ingredient of polarization generation in addition to that arising from the spin-orbit coupling associated with the Mn spiral spin order, may apply beyond DMO.

The above addressed physics can explain the  $H$ -response of  $P$  too. For DMO, a field  $H$  can transform the independent Dy order into the Dy spiral spin order.<sup>5,7</sup> The reoccurrence of the latter is directly linked to the  $H$ -induced enhancement of  $P$  below  $T_{Dy}$ , as shown in Fig. 4(b).<sup>5,7,9</sup> This effect has its maximal at  $H \sim 20$  kOe and then is gradually suppressed upon further increasing  $H$ , responsible for the first positive and then negative  $\Delta P$  as a function of  $H$ . For the case of Ho-substitution,  $P$  always decays against increasing  $H$  due to the continuous suppression of both the Mn spiral spin order and the induced Dy/Ho spiral spin order. It is therefore reasonable to conclude that the rare earth spin order does play a major role in modulating the response of  $P$  to  $H$ . Indeed, upon the Ho-substitution, a slight shift of the  $P$ - $T$  curve towards the low- $T$  side around  $T_{FE}$  is observed (Fig. 4(a)). This behavior is consistent with the variation of the  $C/T \sim T$  curve with increasing  $x$  (Fig. 3(b)).

It should be mentioned that  $P_{so}$  and  $P_{sp}$ , arising, respectively, from the spin-orbit coupling (term  $\langle S_i \times S_j \rangle_{Mn}$ ) and from the spin-lattice coupling (term  $[S_R \cdot S_{Mn}]$ ), may not align

along the same orientation as a general rule.<sup>3</sup> Therefore,  $P = P_{so} + P_{sp}$  as an explicit expression may not be true for single crystals. Here we consider the polycrystalline samples without preferred texture or orientation, and this expression remains acceptable.

In summary, we have investigated the multiferroic behaviors of partial Ho-substituted  $DyMnO_3$ . It is revealed that a proper Ho-substitution of Dy can effectively suppress the independent Dy spin order at low  $T$  but maintain the strong  $R$ -Mn spin coupling so that the polarization at low  $T$  can be remarkably enhanced. The present work approves the capability to combine the various contributions to ferroelectricity in order to enhance the polarization on one hand, and on the other hand further demonstrates the  $R$ -Mn spin coupling as an ingredient of the physics for polarization generation in multiferroic  $RMnO_3$  beyond  $DyMnO_3$ .

This work was supported by the Natural Science Foundation of China (50832002, 11004027, and 51021091), the National Key Projects for Basic Research of China (2009CB929501 and 2009CB623303).

<sup>1</sup>M. Fiebig, *J. Phys. D* **38**, R123 (2005); K. F. Wang, J.-M. Liu, and Z. F. Ren, *Adv. Phys.* **58**, 321 (2009).

<sup>2</sup>T. Kimura, T. Goto, H. Shintani, K. Ishizaka, T. Arima, and Y. Tokura, *Nature (London)* **426**, 55 (2003); W. Eerenstein, N. D. Mathur, and J. F. Scott, *ibid.* **442**, 759 (2006).

<sup>3</sup>B. Lorenz, Y. Q. Wang, and C.-W. Chu, *Phys. Rev. B* **76**, 104405 (2007); N. Lee, Y. J. Choi, M. Ramazanoglu, W. Ratcliff II, V. Kiryukhin, and S. W. Cheong, *ibid.* **84**, 020101 (2011).

<sup>4</sup>R. Feyerherm, E. Dudzik, N. Aliouane, and D. N. Argyriou, *Phys. Rev. B* **73**, 180401(R) (2006).

<sup>5</sup>O. Prokhnenko, R. Feyerherm, E. Dudzik, S. Landsgesell, N. Aliouane, L. C. Chapon, and D. N. Argyriou, *Phys. Rev. Lett.* **98**, 057206 (2007).

<sup>6</sup>N. Aliouane, O. Prokhnenko, R. Feyerherm, M. Mostovoy, J. Stempfer, K. Habicht, K. Rule, E. Dudzik, A. U. B. Wolter, A. Maljuk, and D. N. Argyriou, *J. Phys.: Condens. Matter* **20**, 434215 (2008).

<sup>7</sup>R. Feyerherm, E. Dudzik, A. U. B. Wolter, S. Valencia, O. Prokhnenko, A. Maljuk, S. Landsgesell, N. Aliouane, L. Bouchenoire, S. Brown, and D. N. Argyriou, *Phys. Rev. B* **79**, 134426 (2009).

<sup>8</sup>E. Schierle, V. Soltwisch, D. Schmitz, R. Feyerherm, A. Maljuk, F. Yokai-chiya, D. N. Argyriou, and E. Weschke, *Phys. Rev. Lett.* **105**, 167207 (2010).

<sup>9</sup>R. Feyerherm, E. Dudzik, O. Prokhnenko, and D. N. Argyriou, *J. Phys.: Conf. Ser.* **200**, 012032 (2010).

<sup>10</sup>J. Hemberger, F. Schrettle, A. Pimenov, P. Lunkenheimer, V. Yu. Ivanov, A. A. Mukhin, A. M. Balbashov, and A. Loidl, *Phys. Rev. B* **75**, 035118 (2007).

<sup>11</sup>Y. Yamasaki, S. Miyasaka, T. Goto, H. Sagayama, T. Arima, and Y. Tokura, *Phys. Rev. B* **76**, 184418 (2007).

<sup>12</sup>M. Mochizuki and N. Furukawa, *Phys. Rev. B* **80**, 134416 (2009).

<sup>13</sup>J. A. Moreira, A. Almeida, W. S. Ferreira, J. P. Araújo, A. M. Pereira, M. R. Chaves, M. M. R. Costa, V. A. Khomchenko, J. Kreisel, D. Chernyshov, S. M. F. Vilela, and P. B. Tavares, *Phys. Rev. B* **82**, 094418 (2010).

<sup>14</sup>I. A. Sergienko and E. Dagotto, *Phys. Rev. B* **73**, 094434 (2006); H. Katsura, N. Nagaosa, and A. V. Balatsky, *Phys. Rev. Lett.* **95**, 057205 (2005).

<sup>15</sup>S. Ishiwata, Y. Kaneko, Y. Tokunaga, Y. Taguchi, T. Arima, and Y. Tokura, *Phys. Rev. B* **81**, 100411(R) (2010).

<sup>16</sup>S. Dong, R. Yu, S. Yunoki, J.-M. Liu, and E. Dagotto, *Phys. Rev. B* **78**, 155121 (2008); Q. C. Li, S. Dong, and J.-M. Liu, *Phys. Rev. B* **77**, 054442 (2008).

<sup>17</sup>S. J. Luo, K. F. Wang, S. Z. Li, X. W. Dong, Z. B. Yan, H. L. Cai, and J.-M. Liu, *Appl. Phys. Lett.* **94**, 172504 (2009).

<sup>18</sup>N. Zhang, S. Dong, G. Q. Zhang, L. Lin, Y. Y. Guo, J.-M. Liu, and Z. F. Ren, *Appl. Phys. Lett.* **98**, 012510 (2011).